

Article

Assessment of Cytotoxicity of Magnesium Oxide and Magnesium Hydroxide Nanoparticles using the Electric Cell-Substrate Impedance Sensing

Manishi Pallavi ^{1,2,3}, Jenora Waterman ⁴ , Youngmi Koo ^{2,3}, Jagannathan Sankar ^{2,5}
and Yeohung Yun ^{2,3,*}

¹ Department of Energy and Environmental Systems, North Carolina Agricultural and Technical State University, Greensboro, NC 27411, USA; mpallavi@aggies.ncat.edu

² Engineering Research Center for Revolutionized Metallic Biomaterials, North Carolina Agricultural and Technical State University, Greensboro, NC 27411, USA; kooy20120503@gmail.com (Y.K.); sankar@ncat.edu (J.S.)

³ Department of Chemical, Biological and Bioengineering, North Carolina Agricultural and Technical State University, Greensboro, NC 27411, USA

⁴ Department of Animal Sciences, North Carolina Agricultural and Technical State University, Greensboro, NC 27411, USA; jdwaterm@ncat.edu

⁵ Department of Mechanical Engineering, North Carolina Agricultural and Technical State University, Greensboro, NC 27411, USA

* Correspondence: yun@ncat.edu

Received: 2 March 2020; Accepted: 18 March 2020; Published: 20 March 2020



Abstract: Magnesium (Mg)-based alloys have the potential for bone repair due to their properties of biodegradation, biocompatibility, and structural stability, which can eliminate the requirement for a second surgery for the removal of the implant. Nevertheless, uncontrolled degradation rate and possible cytotoxicity of the corrosion products at the implant sites are known current challenges for clinical applications. In this study, we assessed in vitro cytotoxicity of different concentrations (0 to 50 mM) of possible corrosion products in the form of magnesium oxide (MgO) and magnesium hydroxide (Mg(OH)₂) nanoparticles (NPs) in human fetal osteoblast (hFOB) 1.19 cells. We measured cell proliferation, adhesion, migration, and cytotoxicity using a real-time, label-free, non-invasive electric cell-substrate impedance sensing (ECIS) system. Our results suggest that 1 mM concentrations of MgO/Mg(OH)₂ NPs are tolerable in hFOB 1.19 cells. Based on our findings, we propose the development of innovative biodegradable Mg-based alloys for further in vivo animal testing and clinical trials in orthopedics.

Keywords: cytotoxicity; human fetal osteoblast (hFOB) 1.19 cells; electric cell-substrate impedance sensing (ECIS) system

1. Introduction

Magnesium (Mg)-based alloy has a potential advantage as a biodegradable material due to its biocompatibility and structural stability in orthopedic implant applications [1]. The biodegradable implant degrades in the physiological environment of the body after healing the diseased tissues and bone fractures [2]. Thus, it can eliminate a need for a second surgery to remove the implant. However, studies suggest that Mg-based screws and plates corrode at a very fast rate in an in vivo environment, producing subcutaneous gas cavities [3,4]. Disparity between in vitro and in vivo study results are also reported due to the different corrosive environments [5,6]. Therefore, there is a requirement to

understand the cytotoxicity of the possible corrosion products for the future development of innovative Mg-based alloys in orthopedics [7].

Magnesium (Mg^{2+}) is the most important bivalent ion associated with the physiological functions of the body and participates actively in maintaining the cellular homeostasis [8–10]. Magnesium partakes in more than 300 biochemical reactions, mostly associated with the regulation of ion channels, intracellular signaling, and oxidative phosphorylation [11]. Studies suggest that approximately 53% of total body magnesium is stored in the bones [12–17]. Deficiency of magnesium affects the metabolism of the skeleton, which inhibits bone growth and formation of new osteoblast cells, resulting in bone brittleness [8,18–28]. There are many study reports on Mg-based biodegradable orthopedic implants; however, the real-time concentration-based toxicity of the corrosion products in the form of magnesium oxide (MgO) and magnesium hydroxide ($Mg(OH)_2$) nanoparticles (NPs) that might be released during the implant degradation process is not known.

In this study, we assessed the cytotoxicity of randomly selected different concentrations (0, 1, 5, 10, and 50 mM) of MgO/ $Mg(OH)_2$ NPs in hFOB 1.19 cells [7] using a real-time electric cell-substrate impedance sensing (ECIS) system. With this ECIS system, cell adhesion and proliferation have been evaluated quantitatively by the generated impedance relative to the time to measure the cytotoxicity. Studies suggest that bone hemostasis is affected by the pH [29]; therefore, this study also assessed the change in the pH to measure the cytotoxicity in hFOB 1.19 cells in response to the different concentrations of MgO/ $Mg(OH)_2$ NPs. As an outcome of this novel real-time in vitro ECIS study, we report our findings for an allowable concentration of MgO/ $Mg(OH)_2$ NPs that might be released from Mg-based biodegradable alloys for its applications in future in vivo studies of orthopedic implants.

2. Materials and Methods

2.1. Materials

We purchased magnesium oxide nanoparticles (MgO NPs) (nanopowder, < 50 nm particle size; Cat# 549649-5G) and magnesium hydroxide nanoparticles ($Mg(OH)_2$ NPs) (nanopowder, < 100 nm particle size; Cat# 632309-25G) from Sigma-Aldrich, Milwaukee, WI, USA, based on our previous study [7]. Before conducting ECIS experiments, MgO/ $Mg(OH)_2$ NPs were sterilized through ultraviolet (UV) rays [7].

2.2. Cell Culture

In our experiments, a human osteoblast hFOB 1.19 cell line (SV40 large T antigen transfected; American Type Culture Collection) (Cat# ATCC®CRL-11372™, Manassas, VA, USA) were cultured in complete growth media based on our previous study [7]. Complete growth medium contained a 1:1 mixture of Ham's F12 medium with L-glutamine (Cat#10-080-CV, Cellgro, Manassas, VA, USA) and Dulbecco's Modified Eagle's Medium with 4.5 g/L glucose and sodium pyruvate without L-glutamine and phenol red (Cat# 17-205-CV, Cellgro, Manassas, VA, USA), supplemented with 0.3 mg/mL gentamicin sulfate (Cat# 17-518Z, Lonza, Walkersville, MD, USA) and 10% fetal bovine serum (heat-inactivated at 56 °C) (Cat# S1105H, Atlanta Biologicals, Flowery Branch, GA, USA) [7]. Cells were maintained under standard cell culture conditions (37 °C, 5% CO_2) with humidified air and were utilized after three passages [7].

2.3. Impedance Measurement

ECIS system was utilized to study the concentration-based cytotoxicity of MgO/ $Mg(OH)_2$ NPs in hFOB 1.19 cells [7] as an alternative to the trial-and-error of animal testing. Here, array type 8W1E PET (Applied Biophysics, NY, USA) consisting of eight wells, each well with a single circular 250 μ m diameter active gold electrode, was used for ECIS. Arrays were attached to the ECIS system (Model ECIS Z0, Applied Biophysics, NY, USA), and alternative current (I) of 4000 Hz was applied to the eight-well sensing electrodes. A voltage (V) across the electrodes created an impedance (Z), which

was measured by Ohm's law ($Z = V/I$). With the morphological changes in hFOB 1.19 cells in response to different concentrations of MgO/Mg(OH)₂ NPs [7] in the arrays, impedance was measured.

After the third passage of the hFOB 1.19 cells in a complete growth media, 400 μ L of the cells (5000 cells/well) were seeded in two sets of eight-well arrays for control and experimental groups. Arrays were incubated under standard cell culture conditions (37 °C, 5% CO₂) with humidified air for 24 h [7]. After 24 h, different concentrations (0, 1, 5, 10, and 50 mM) of MgO/Mg(OH)₂ NPs [7] were exposed to the respective wells of the arrays, followed by incubation for another 24 h. Impedance was measured after 24 h of MgO/Mg(OH)₂ NP exposure.

2.4. Fluorescence Microscope

The digital inverted fluorescence microscope (EVOS XL, Life Technologies) was utilized to observe the live images of hFOB 1.19 cells upon exposure to MgO/Mg(OH)₂ NPs for 24 h on the microelectrodes of the arrays. The fluorescence microscope was utilized because of the unique high resolution and high sensitivity of the camera.

2.5. The pH Measurement

After treating the hFOB 1.19 cells with different concentrations of MgO/Mg(OH)₂ NPs, pH values of the control and experimental groups was measured at 24 h. The pH values were measured with a pH meter (Oakton®pH2100, Eutech Instruments, Singapore) to evaluate the cytotoxicity of MgO/Mg(OH)₂ NPs in a time- and concentration-dependent manner.

2.6. Statistical Analysis

Impedance with respect to time was measured by the one-way analysis of variance (ANOVA) technique by GraphPad Prism version 5.0 software (GraphPad Software, Inc., San Diego, CA). The change in the pH of media of control and experimental groups for MgO/Mg(OH)₂ NPs were also statistically analyzed by one-way ANOVA techniques. Data are presented as mean \pm SEM.

3. Results and Discussion

A real-time ECIS monitoring was used for assessing the cytotoxicity of different concentrations (0, 1, 5, 10, and 50 mM) of MgO/Mg(OH)₂ NPs in hFOB 1.19 cells. With this sensitive and robust system, impedance was generated with respect to the time to quantify the morphological changes in hFOB 1.19 cells after the treatment. This result provides an allowable concentration of MgO/Mg(OH)₂ NPs in hFOB 1.19 cells. Based on these real-time study results, we propose the development of sustainable, biodegradable Mg-based alloys for future in vivo testing in orthopedics.

3.1. The Confluence of hFOB Osteoblast Cells

Osteoblast differentiation is observed by the stages of cell proliferation, matrix maturation, and mineralization [30]. In addition, in vitro matrix maturation and mineralization increase with the complete confluence of the cells [31].

The results illustrated in Figure 1 shows that after seeding hFOB 1.19 cells for 24 h, the size of the cells changed from round to elongated due to cell differentiation and maturation, and there was approximately 20–30% confluency. After the first passage, cells were proportionately spread and approximately 30–40% confluent with a few dead cells at 48 h. After the second passage, cells were spread and approximately 50–60% confluent, with a reduced number of the dead cells at 72 h. However, after the third passage, cells were elongated, spread, and approximately 70–90% confluent, with a negligible number of dead cells at 96 h. These optimally confluent hFOB 1.19 cells provided a suitable condition for the assessment of cytotoxicity upon exposure to different concentrations of MgO/Mg(OH)₂ through the real-time ECIS monitoring system.

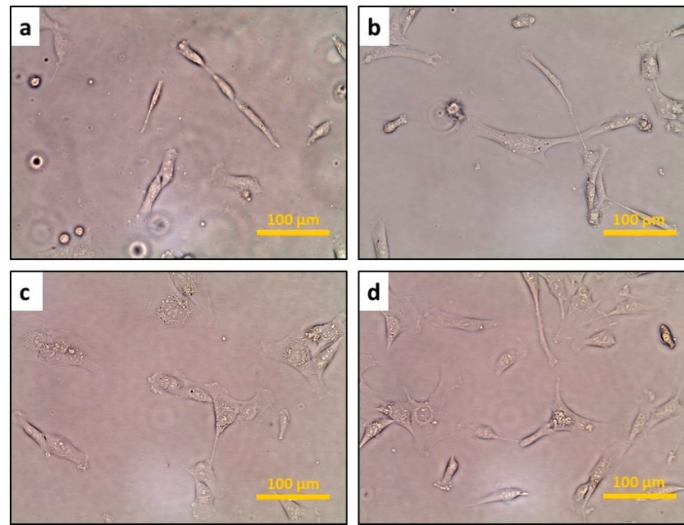


Figure 1. Confluence of human fetal osteoblast (hFOB) 1.19 cells cultured in complete growth media at different time points: (a) 20–30% of cell confluence at 24 h; (b) 30–40% of cell confluence at 48 h; (c) 50–60% of cell confluence at 72 h; and (d) 70–90% of cell confluence at 96 h of seeding.

3.2. The Response of hFOB Osteoblast Cells on ECIS after Treatment

The images of hFOB 1.19 cells after treatment with different concentrations (0, 1, 5, 10, and 50 mM) of MgO and Mg(OH)₂ NPs at 24 h on a transparent single circular 250 µm diameter active gold electrode of the ECIS system are shown in Figures 2 and 3, respectively. Results in Figure 2 show that after treating hFOB 1.19 cells with 0 mM of MgO NPs at 24 h, cells proliferate, spread, and adhere to the electrode, maintaining a confluent monolayer. At the lower concentration (1 mM) of MgO NPs, hFOB 1.19 cells show similar proliferation as that of the control group (0 mM), representing normal hemostasis of the cells. However, at the concentrations of 5, 10, and 50 mM of MgO NPs, the subsequent reduction in cell number was observed.

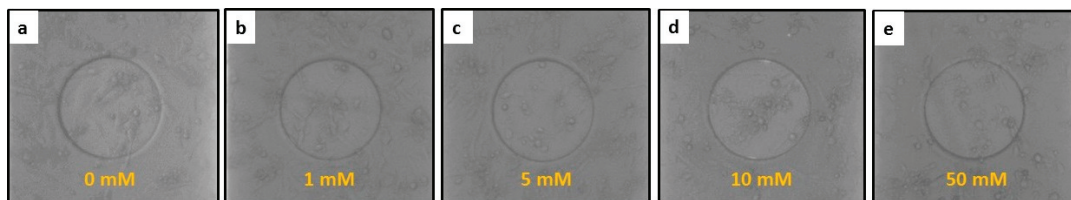


Figure 2. Images of live and dead hFOB 1.19 cells on microfabricated electrodes after treatment with different concentrations of MgO nanoparticles (NPs) at 24 h: (a) 0 mM MgO NPs (control group); (b) 1 mM MgO NPs; (c) 5 mM MgO NPs; (d) 10 mM MgO NPs; and (e) 50 mM MgO NPs.

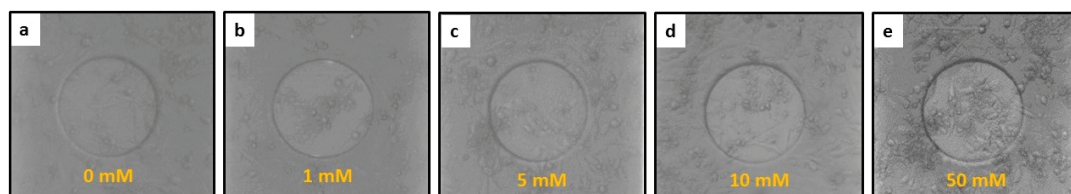


Figure 3. Images of live and dead hFOB 1.19 osteoblast cells on microfabricated electrodes after treatment with different concentrations of Mg(OH)₂ NPs at 24 h: (a) 0 mM Mg(OH)₂ (control group); (b) 1 mM Mg(OH)₂; (c) 5 mM Mg(OH)₂; (d) 10 mM Mg(OH)₂; and (e) 50 mM Mg(OH)₂.

Results in Figure 3 show that after treating hFOB 1.19 cells with 0 mM of $\text{Mg}(\text{OH})_2$ NPs at 24 h, cells proliferate, spread, and adhere to the electrode and maintain the uniform monolayer. At the lower concentration (1 mM) of $\text{Mg}(\text{OH})_2$ NPs, hFOB 1.19 cells show adhesion; however, the reduction in cell growth was observed as compared to the control group (0 mM). With the concentrations of 5 and 10 mM of $\text{Mg}(\text{OH})_2$ NPs, subsequent reduction in cell growth and number of the live cells was observed. With the exposure of the 50 mM concentration of $\text{Mg}(\text{OH})_2$ NPs on the hFOB 1.19 cells, a drastic reduction in the cell growth was observed.

Comparing the reactivity of hFOB 1.19 cells in response to the exposure of 50 mM concentrations of MgO and $\text{Mg}(\text{OH})_2$ NPs for 24 h, results depict major reduction in cell proliferation and spread for $\text{Mg}(\text{OH})_2$ NPs.

3.3. ECIS Measurement

ECIS results are shown in Figures 4 and 5 in response to the exposure of different concentrations (0, 1, 5, 10, and 50 mM) of MgO/ $\text{Mg}(\text{OH})_2$ NPs, respectively, on hFOB 1.19 cells. Cells were utilized after three passages to obtain high throughput results through ECIS experiments. Cells were incubated for 24 h on microelectrodes of the ECIS array for the control group (0 mM) and the experimental groups (1, 5, 10, and 50 mM) to evaluate the cytotoxicity of different concentrations of MgO/ $\text{Mg}(\text{OH})_2$ NPs upon exposure. Figures 4 and 5 illustrate an increase in impedance at 24 h due to the cell proliferation and formation of the monolayer of the cells. Further, a drop in the impedance for an hour has been observed after 24 h in the samples due to the change of the culture media of the control group and the experimental groups before exposure of the concentrations of MgO/ $\text{Mg}(\text{OH})_2$ NPs.

Figure 4 shows the ECIS impedance response to hFOB 1.19 cells upon exposure of different concentrations of MgO NPs for 24 h. At a 0 mM concentration of MgO NPs, a constant monolayer of cells was observed due to rapid cell proliferation, resulting in an increase impedance that saturated at 8700 Ω after 24 h. For the lower concentration (1 mM) of MgO NPs, increased cell proliferation and formation of a monolayer of cells have been observed, which resulted in an increased impedance that saturated at 8600 Ω after 24 h. Nearly similar impedance results for 1 mM concentrations of MgO NPs and control group (0 mM) indicates the negligible amount of cytotoxicity to the hFOB 1.19 cells. However, at concentrations of 5, 10, and 50 mM, a subsequent decrease in the impedance to 8300.4, 8200, and 8080 Ω was reported, respectively, as compared to control group (0 mM) and 1 mM concentration of MgO NPs. The decrease in impedance demonstrates increased cytotoxicity in hFOB 1.19 cells, mainly due to cell death that has been confirmed with the live-cell images of hFOB 1.19 cells on microelectrodes upon exposure, as shown in Figure 2.

Figure 5 shows the ECIS impedance response to hFOB 1.19 cells upon exposure to different concentrations (0, 1, 5, 10, and 50 mM) of $\text{Mg}(\text{OH})_2$ NPs for 24 h. At 0 mM concentration, a constant monolayer of cells was identified with rapid cell proliferation with an increase of impedance that saturated at 8400 Ω after 24 h. Exposure to a lower concentration, such as 1 mM, cell proliferation and formation of a monolayer of cells with an increased impedance that saturated at 8130 Ω after 24 h was observed. However, at the concentrations of 5, 10, and 50 mM, subsequent decreases in the impedance to 7890, 7830, and 7810 Ω were reported, respectively, as compared to control group (0 mM) and 1 mM concentrations of $\text{Mg}(\text{OH})_2$ NPs. A subsequent decrease in the impedance results reveals increased cytotoxicity with the higher concentrations of 5, 10, and 50 mM of $\text{Mg}(\text{OH})_2$ NPs. Cytotoxicity was also confirmed with the live-cell images of hFOB 1.19 cells on microelectrodes upon exposure, as shown in Figure 3. To access the level of cytotoxicity among the different concentrations of MgO and $\text{Mg}(\text{OH})_2$ NPs for 24 h, ECIS impedance responses of hFOB 1.19 cells upon exposure have been compared. The combined results of ECIS impedance and the live images depict that 1 mM concentrations of MgO NPs are less toxic to hFOB 1.19 cells as compared to 1 mM concentrations of $\text{Mg}(\text{OH})_2$ NPs.

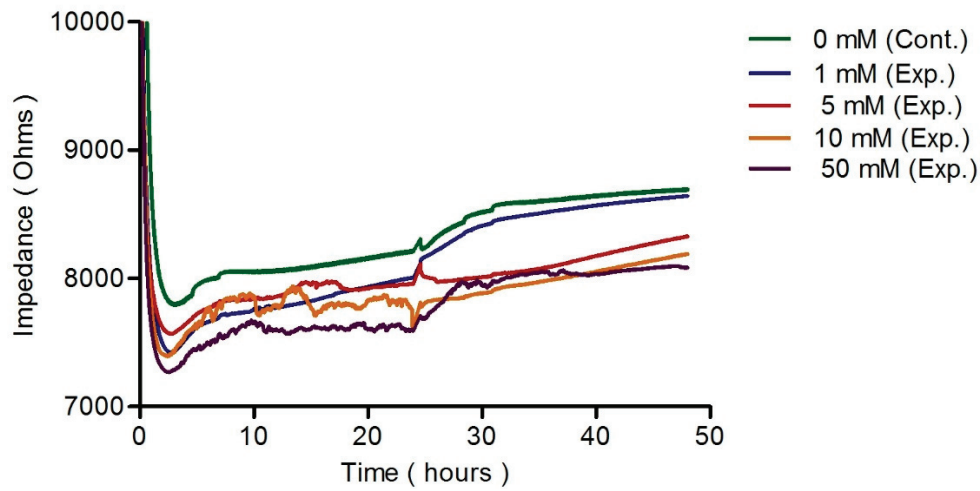


Figure 4. Real-time electric cell-substrate impedance sensing (ECIS) impedance results measuring cytotoxicity in hFOB 1.19 cells in response to different concentrations of MgO NPs.

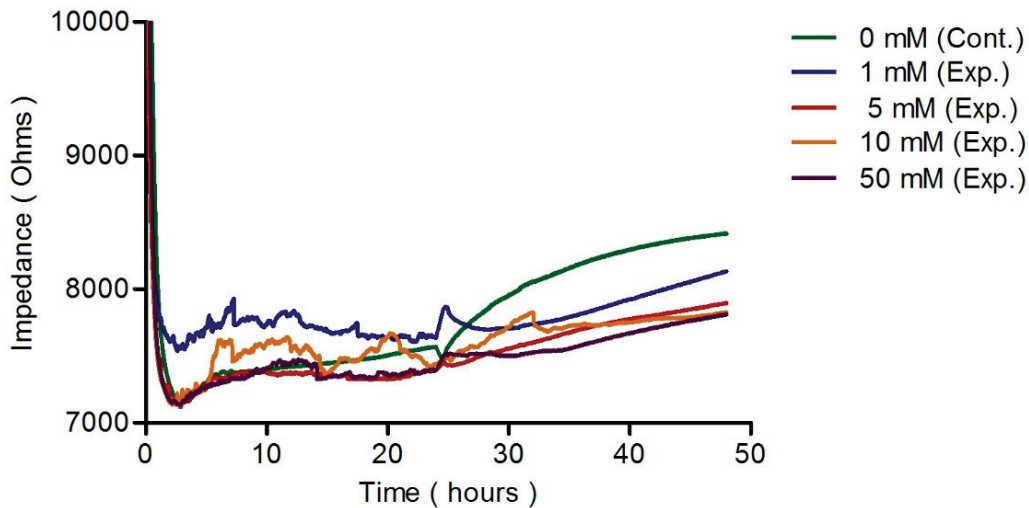


Figure 5. Real-time ECIS impedance results measuring cytotoxicity in hFOB 1.19 cells in response to different concentrations of Mg(OH)₂ NPs.

3.4. Analysis of the pH Changes

Figure 6 shows the change in pH of hFOB 1.19 cells after exposure with different concentrations (0, 1, 5, 10, and 50 mM) of MgO NPs. Results show that with the increasing concentrations of MgO NP exposures in hFOB 1.19 cells, the pH was more alkaline (mean pH values: 1 mM = 7.83, 5 mM = 8.13, 10 mM = 8.33, 50 mM = 8.83) when compared to the control group (0 mM = 7.53).

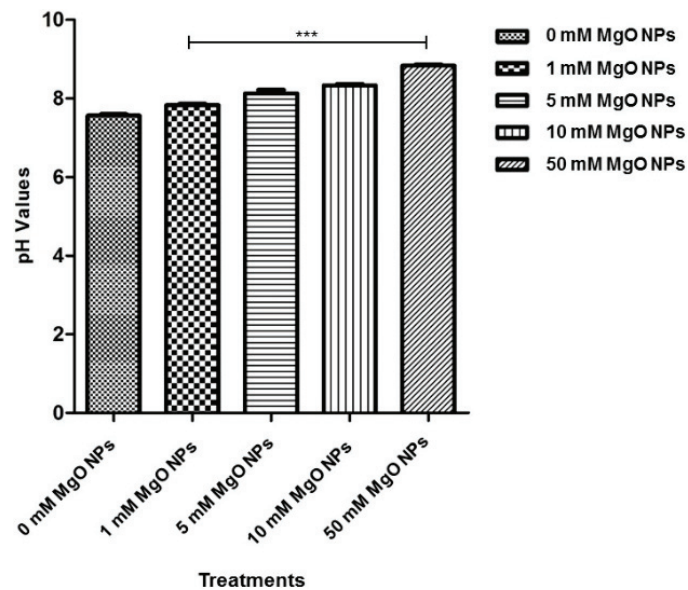


Figure 6. Analysis of the change in pH in hFOB 1.19 cells in response to the different concentrations of MgO NPs. Data are obtained as means \pm SEM, $n = 3$; *** p -value ≤ 0.0001 when compared to the control group.

Figure 7 shows that with the increasing concentrations of $\text{Mg}(\text{OH})_2$ NPs exposure in hFOB 1.19 cells, the pH was more alkaline (mean pH values: 1 mM = 8.23, 5 mM = 8.33, 10 mM = 8.57, 50 mM = 9.07) when compared to the control group (0 mM = 7.57).

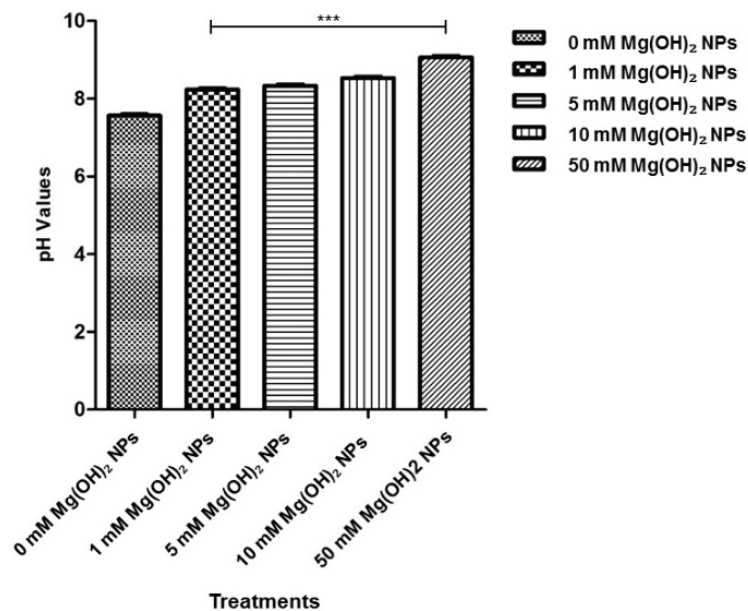


Figure 7. Analysis of the change in pH in hFOB 1.19 cells in response to the different concentrations of $\text{Mg}(\text{OH})_2$ NPs. Data are obtained as means \pm SEM, $n = 3$; *** p -value ≤ 0.0001 when compared to the control group.

3.5. Discussion

Mg-based biodegradable orthopedic implants dissolve in the physiological environment of the body, producing corrosion products [3,4]. Studies suggest that the degradation behavior of the Mg-based implants varies due to different corrosive environments of *in vitro* and *in vivo* studies [5], which makes it challenging to establish Mg as a next-generation biodegradable material [3,7]. Therefore, in this study, we used a real-time ECIS system to mimic the *in vivo* environment for assessing the cytotoxicity of different concentrations (0, 1, 5, 10, and 50 mM) of MgO/Mg(OH)₂ NPs in hFOB 1.19 cells [7]. Based on our findings by real-time ECIS study, we propose the development of sustainable, biodegradable Mg-based alloys as the implant materials for orthopedic applications.

Osteoblast differentiation progresses by the process of cell proliferation, matrix maturation, and mineralization [30]. In the case of the *in vitro* environment, the complete confluence of the cells increases matrix maturation and mineralization [31]. Magnesium homeostasis and regulation of cell functions such as cell proliferation, energy metabolism, and the apoptosis process in healthy and diseased cells are also reported [32]. Therefore, in our study, we investigated the confluence of the hFOB 1.19 cells for 24, 48, 72, and 96 h [7] before ECIS experiments. Results show that after 96 h, cells were approximately 70–80% confluent with a negligible number of dead cells when compared to 72 (50–60% confluence), 48 (30–40% confluence), and 24 h (20–30% confluence). The maximum convergence of hFOB 1.19 cells significantly contributes to avoiding any false-positive results with dead cells that might otherwise interfere with the ECIS impedance upon exposure to MgO/Mg(OH)₂ NPs [7].

The ECIS impedance result reveals that 1 mM concentrations of MgO NPs provide a similar range of impedance as the control group (0 mM), which indicates magnesium homeostasis, as shown in Figure 4. However, at the subsequent higher concentrations, such as 5, 10, and 50 mM concentrations of MgO NPs [7], the impedance drops significantly, indicating cytotoxicity by inhibiting cell proliferation. Comparative impedance results of MgO and Mg(OH)₂ NPs [7] in Figures 4 and 5, respectively, show that impedance is lower at 50 mM concentrations of Mg(OH)₂ NPs [7] when compared to MgO NPs [7], which indicates high cytotoxicity of Mg(OH)₂ at 50 mM. These results have been confirmed by the images of live and dead cells on microfabricated electrodes in Figures 2 and 3, respectively.

Studies suggest that extracellular pH and oxygen tension alters the bone hemostasis [29]. Besides, the skeleton serves as the reservoir of alkaline mineral (hydroxyapatite), which releases in case of metabolic acid-base imbalance [33]. Also, reports on bone cells suggest that at acidic pH, osteoblast activity inhibits, which results in inhibition of mineral deposition [29,33]. However, the bone resorption activity of osteoclast cells gets activated at acidic pH [33]. The changes in pH levels of the possible corrosion products are not entirely understood. Therefore, with this study, insight into the change in pH of different concentrations of MgO/Mg(OH)₂ NPs upon exposure to hFOB 1.19 cells [7] has also been gained.

Little evidence of the *in vitro* test to study the cytotoxicity of the corrosion products is reported [7]. However, in this study, we provide real-time *in vitro* ECIS results for an allowable concentration of MgO/Mg(OH)₂ NPs in hFOB 1.19 cells. With the results obtained from our study, we propose the development of sustainable, biodegradable Mg-based alloys for future *in vivo* testing for orthopedic implant applications.

4. Conclusions

Mg-based orthopedic implants have an added advantage due to their biodegradation behavior, which can eliminate the requirement of a second surgery to remove implant after they support, repair, and heal bones. However, cytotoxicity of the possible corrosion products in the form of MgO/Mg(OH)₂ NPs that might be released during the process of implant degradation is not entirely understood. Currently, little evidence of *in vitro* assessment of the cytotoxicity of the possible corrosion products in osteoblast cells has been reported [7]. Conversely, there is a need to assess the cytotoxicity of the potential corrosion products in a real-time manner for the future development of sustainable,

biodegradable Mg-based alloys for in vivo animal testing and clinical trials in orthopedics. Therefore, in our study, we assessed the cytotoxicity of different concentrations (0, 1, 5, 10, and 50 mM) of MgO/Mg(OH)₂ NPs in hFOB 1.19 cells [7] using a real-time ECIS monitoring system. Our results show that 1 mM concentrations of MgO/Mg(OH)₂ NPs are an allowable concentration in hFOB 1.19 cells. We propose the development of sustainable, biodegradable Mg-based alloys for future in vivo animal testing and clinical trials for commercial application in the orthopedic implants industry.

Author Contributions: Conceptualization, Y.Y. and J.W.; methodology, Y.K.; software, M.P., validation, M.P. and Y.Y.; formal analysis M.P. and Y.Y., Investigation, M.P.; Resources, J.S.; data curation, M.P.; writing—original draft preparation, M.P.; writing—review and editing, Y.Y., M.P., and J.W.; visualization, M.P.; supervision, Y.Y. and J.S.; project administration, J.W. and J.S.; funding acquisition, Y.Y. and J.S. [7]. All authors have read and agreed to the published version of the manuscript.

Funding: This research received funding from the National Science Foundation Engineering Research Center for Revolutionizing Metallic Biomaterials, NIH grant (GM113728), ARO grant (74386), and NSF grant (1649243) [7].

Conflicts of Interest: The authors declare no conflict of interest.

References

1. Witte, F.; Kaese, V.; Haferkamp, H.; Switzer, E.; Meyer-Lindenberg, A.; Wirth, C.J.; Windhagen, H. In vivo corrosion of four magnesium alloys and the associated bone response. *Biomaterials* **2005**, *26*, 3557–3563. [[CrossRef](#)] [[PubMed](#)]
2. Staiger, M.P.; Pietak, A.M.; Huadmai, J.; Dias, G. Magnesium and its alloys as orthopedic biomaterials: A review. *Biomaterials* **2006**, *27*, 1728–1734. [[CrossRef](#)] [[PubMed](#)]
3. McBride, E.D. Absorbable metal in bone surgery. *J. Am. Med. Assoc.* **1938**, *111*, 2464–2467. [[CrossRef](#)]
4. Verbrugge, J. Le Mate' riel Me' tallique Re' sorbable En Chirurgie Osseuse. *La Press Med.* **1934**, *23*, 460–465.
5. Williams, D.F. Effects of the environment on materials. *Biomed. Eng.* **1971**, *6*, 106–113. [[PubMed](#)]
6. Witte, F.; Fischer, J.; Nellesen, J.; Crostack, H.A.; Kaese, V.; Pisch, A.; Beckmann, F.; Windhagen, H. In vitro and in vivo corrosion measurements of magnesium alloys. *Biomaterials* **2006**, *27*, 1013–1018. [[CrossRef](#)] [[PubMed](#)]
7. Pallavi, M.; Waterman, J.; Koo, Y.; Sankar, J.; Yun, Y. In Vitro Cytotoxicity of Possible Corrosion Products from Mg-Based Biodegradable Metals: Magnesium Oxide and Magnesium Hydroxide Nanoparticles. *Appl. Sci.* **2019**, *9*, 4304. [[CrossRef](#)]
8. Günther, T. Comment on the number of magnesium activated enzymes. *Magnes. Res.* **2008**, *1*, 185–187.
9. Rubin, H. Magnesium: The missing element in molecular views of cell proliferation control. *Bioessays*. **2005**, *27*, 311–320. [[CrossRef](#)]
10. Yun, Y.; Dong, Z.; Lee, N.; Liu, Y.; Xue, D.; Guo, X.; Kuhlmann, J.; Doepke, A.; Halsall, H.B.; Heineman, W.; et al. Revolutionizing biodegradable metals. *Mater. Today* **2009**, *12*, 22–32. [[CrossRef](#)]
11. McCarthy, T.J.; Kumar, R. Divalent Cation Metabolism: Magnesium. In *Atlas of Diseases of the Kidney*; Schrier, R.W., Ed.; Blackwell Science: Malden, MA, USA, 1999; pp. 4.1–4.8.
12. Al-Ghamdi, S.M.G.; Cameron, E.C.; Sutton, R.A.L. Magnesium deficiency: Pathophysiologic and clinical overview. *Am. J. Kidney Dis.* **1994**, *24*, 737–752. [[CrossRef](#)]
13. De Rouffignac, C.; Quamme, G. Renal magnesium handling and its hormonal control. *Physiol. Rev.* **1994**, *74*, 305–322. [[CrossRef](#)] [[PubMed](#)]
14. McLean, R.M. Magnesium and its therapeutic uses: A review. *Am. J. Med.* **1994**, *96*, 63–76. [[CrossRef](#)]
15. Quamme, G.A. Magnesium homeostasis and renal magnesium handling. *Miner. Electrolyte Metab.* **1993**, *19*, 218–225.
16. Nadler, J.L.; Rude, R.K. Disorders of magnesium metabolism. *Endocrin. Metab. Clin.* **1995**, *24*, 623–641. [[CrossRef](#)]
17. Whang, R.; Hampton, E.M.; Whang, D.D. Magnesium homeostasis and clinical disorders of magnesium deficiency. *Ann. Pharmacother.* **1994**, *28*, 220–226. [[CrossRef](#)]
18. Abed, E.; Moreau, R. Importance of melastatin-like transient receptor potential 7 and magnesium in the stimulation of osteoblast proliferation and migration by platelet-derived growth factor. *Am. J. Physiol. Cell Phys.* **2009**, *297*, C360–C368. [[CrossRef](#)]
19. Anselme, K. Osteoblast adhesion on biomaterials. *Biomaterials* **2000**, *21*, 667–681. [[CrossRef](#)]

20. Diener, A.; Nebe, B.; Lüthen, F.; Becker, P.; Beck, U.; Neumann, H.G.; Rychly, J. Control of focal adhesion dynamics by material surface characteristics. *Biomaterials* **2005**, *26*, 383–392. [[CrossRef](#)]
21. Hornby, J.E. Measurement of cell adhesion. II. Quantitative study of the effect of divalent ions on cell adhesion. *J. Embryol. Exp. Morph.* **1973**, *30*, 511–518.
22. Li, C.Y.; Gao, S.Y.; Terashita, T.; Shimokawa, T.; Kawahara, H.; Matsuda, S.; Kobayashi, N. In vitro assays for adhesion and migration of osteoblastic cells (Saos-2) on titanium surfaces. *Cell Tissue Res.* **2006**, *324*, 369–375. [[CrossRef](#)] [[PubMed](#)]
23. Maier, J.A.; Bernardini, D.; Rayssiguier, Y.; Mazur, A. High concentrations of magnesium modulate vascular endothelial cell behaviour in vitro. *Biochim. Biophys. Acta.* **2004**, *1689*, 6–12. [[CrossRef](#)] [[PubMed](#)]
24. Moomaw, A.S.; Maguire, M.E. The unique nature of mg²⁺ channels. *Physiology* **2008**, *23*, 275–285. [[CrossRef](#)] [[PubMed](#)]
25. Rouahi, M.; Champion, E.; Hardouin, P.; Anselme, K. Quantitative kinetic analysis of gene expression during human osteoblastic adhesion on orthopaedic materials. *Biomaterials* **2006**, *27*, 2829–2844. [[CrossRef](#)]
26. Spillmann, C.; Osorio, D.; Waugh, R. Integrin activation by divalent ions affects neutrophil homotypic adhesion. *Ann. Biomed. Eng.* **2002**, *30*, 1002–1011. [[CrossRef](#)]
27. Turner, D.; Flier, L.; Carbonetto, S. Magnesium-dependent attachment and neurite outgrowth by PC12 cells on collagen and laminin substrata. *Dev. Biol.* **1987**, *121*, 510–525. [[CrossRef](#)]
28. Zreiqat, H.; Howlett, C.R.; Zannettino, A.; Evans, P.; Schulze-Tanzil, G.; Knabe, C.; Shakibaei, M. Mechanisms of magnesium-stimulated adhesion of osteoblastic cells to commonly used orthopaedic implants. *J. Biomed. Mater. Res.* **2002**, *62*, 175–184. [[CrossRef](#)]
29. Arnett, T.R. Extracellular pH Regulates Bone Cell Function. *J. Nutr.* **2008**, *138*, 415S–418S. [[CrossRef](#)]
30. Stein, G.S.; Lian, J.B. Molecular Mechanisms Mediating Developmental and Hormone-Regulated Expression of Genes in Osteoblasts: An Integrated Relationship of Cell Growth and Differentiation. In *Cellular Molecular Biology of Bone*; Noda, M., Ed.; Academic Press: Tokyo, Japan, 1993; pp. 47–95.
31. Kasperk, C.; Wergedal, J.; Strong, D.; Farley, J.; Wangerin, K.; Gropp, H.; Ziegler, R.; Baylink, D.J. Human bone cell phenotypes differ depending on their skeletal site of origin. *J. Clin. Endocr. Metab.* **1995**, *80*, 2511–2517.
32. Wolf, F.; Trapani, V. Cell (patho) physiology of magnesium. *Clin. Sci.* **2008**, *114*, 27–35. [[CrossRef](#)]
33. Arnett, T.R. Acidosis, hypoxia and bone. *Arch. Biochem. Biophys.* **2010**, *503*, 103–109. [[CrossRef](#)] [[PubMed](#)]



© 2020 by the authors. Licensee MDPI, Basel, Switzerland. This article is an open access article distributed under the terms and conditions of the Creative Commons Attribution (CC BY) license (<http://creativecommons.org/licenses/by/4.0/>).